



HAL
open science

Discrete-time port-Hamiltonian systems: A definition based on symplectic integration

Paul Kotyczka, Laurent Lefevre

► **To cite this version:**

Paul Kotyczka, Laurent Lefevre. Discrete-time port-Hamiltonian systems: A definition based on symplectic integration. *Systems and Control Letters*, 2019, 10.1016/j.sysconle.2019.104530 . hal-02319637

HAL Id: hal-02319637

<https://hal.science/hal-02319637>

Submitted on 18 Oct 2019

HAL is a multi-disciplinary open access archive for the deposit and dissemination of scientific research documents, whether they are published or not. The documents may come from teaching and research institutions in France or abroad, or from public or private research centers.

L'archive ouverte pluridisciplinaire **HAL**, est destinée au dépôt et à la diffusion de documents scientifiques de niveau recherche, publiés ou non, émanant des établissements d'enseignement et de recherche français ou étrangers, des laboratoires publics ou privés.

Discrete-time port-Hamiltonian systems: A definition based on symplectic integration

Paul Kotyczka^{a,*}, Laurent Lefèvre^b

^aTechnical University of Munich, Department of Mechanical Engineering, Chair of Automatic Control, Boltzmannstraße 15,
85748 Garching, Germany

^bUniv. Grenoble Alpes, LCIS, 50 rue Barthélémy de Laffemas, 26902 Valence, France

Abstract

We introduce a new definition of discrete-time port-Hamiltonian systems (PHS), which results from structure-preserving discretization of explicit PHS in time. We discretize the underlying continuous-time Dirac structure with the collocation method and add discrete-time dynamics by the use of symplectic numerical integration schemes. The conservation of a discrete-time energy balance – expressed in terms of the discrete-time Dirac structure – extends the notion of symplecticity of geometric integration schemes to open systems. We discuss the energy approximation errors in the context of the presented definition and show that their order is consistent with the order of the numerical integration scheme. Implicit Gauss-Legendre methods and Lobatto IIIA/IIIB pairs for partitioned systems are examples for integration schemes that are covered by our definition. The statements on the numerical energy errors are illustrated by elementary numerical experiments.

Keywords: Port-Hamiltonian systems, Dirac structures, discrete-time systems, geometric numerical integration, symplectic methods.

1. Introduction

The *geometric* integration of ordinary differential equations, see e.g. [1], [2], is an important approach to perform long-time simulations of Hamiltonian systems. *Symplectic* integration conserves not only the symplectic form in the (mechanical) phase space, but also invariants of motion (Casimirs, first integrals). Symplectic integrators that are derived based on discrete versions of Hamilton's principle are called *variational integrators*. They “work very well for both conservative and dissipative or forced mechanical systems”¹.

The port-Hamiltonian (PH) approach, see [4] for an overview, is very appealing for modeling, simulation and control of complex multiphysics systems. PH systems generalize the *Hamiltonian* system representation by the additional definition of *ports*,

which are pairs of power variables that characterize energy exchange in the system and over its boundary. The numerical integration of PH systems has to account for this energy exchange. Besides the error of the numerical solution itself, the error of the energy transmitted over the *discrete ports* is of fundamental interest in the simulation of PH systems.

Most existing works on the discrete-time formulation of PH systems make use of a *discrete gradient*, defined from a finite-differences point of view ([5], [6], [7]). A generic definition of PH dynamics on discrete manifolds (spaces that locally look like discretization grids or the set of floating-point numbers) is given in [8]. Objects and operations from differential geometry are adapted to the discrete setting and discrete-time Dirac structures are defined. In the discrete setting, the chain rule is not valid, which means that the change of energy over a sampling interval is only *approximated* by a product of the discrete gradient $\partial_x H(x)$ and the increment Δx of the state.

We give a new definition of discrete-time Dirac

*Corresponding author

Email addresses: kotyczka@tum.de (Paul Kotyczka),
laurent.lefevre@lcis.grenoble-inp.fr (Laurent Lefèvre)

¹See [3], Section 2.

structures and discrete-time PHS, which is based on the approximation of the continuous-time structural energy balance and symplectic numerical time integration by *collocation methods*. The corresponding quadrature formulas allow for quantitative statements on the approximation error both of the solution and the supplied energy. We show that only Gauss-Legendre collocation, applied to linear PHS, guarantees an *exact* discrete energy balance as defined in [9], Def. III.2. Our definition includes discretization schemes, which yield a non-exact discrete energy balance. An example are the Lobatto IIIA/IIIB methods for partitioned systems. The energy error is then *consistent with*, i. e. it has the same order as the chosen integration scheme.

The paper is organized as follows. In Section 2, we introduce the considered class of finite-dimensional PH systems and the underlying Dirac structure. Section 3 contains as main results the definitions of discrete-time Dirac structures and PH systems based on the collocation method. In Section 4, we consider Gauss-Legendre methods and Lobatto IIIA/IIIB pairs and discuss the order of the energy approximations. Section 5 illustrates the statements on the elementary example of a linear undamped/damped oscillator. In the concluding Section 6, we sum up the paper, and we point out perspectives for future work based on the presented results.

This paper is inspired by early results on the symplectic time integration of PH systems using Gauss-Legendre collocation [10]. The main novelties are the precise consideration of the different energy approximations, the application of the ideas to more general schemes including s -stage Lobatto pairs for partitioned systems, the analysis and order proofs for the energy errors, and the extended section on numerical experiments.

2. Finite-dimensional PH systems

We consider the class of *lossless* finite-dimensional PH systems in an *explicit* input-state-output representation (see e. g. [4] or [11])

$$\dot{\mathbf{x}}(t) = \mathbf{J}(\mathbf{x}(t))\nabla H(\mathbf{x}(t)) + \mathbf{G}(\mathbf{x}(t))\mathbf{u}(t) \quad (1a)$$

$$\mathbf{y}(t) = \mathbf{G}^T(\mathbf{x}(t))\nabla H(\mathbf{x}(t)) \quad (1b)$$

with state vector $\mathbf{x} \in \mathbb{R}^n$, collocated in- and output vectors $\mathbf{u}, \mathbf{y} \in \mathbb{R}^m$. The Hamiltonian $H : \mathbb{R}^n \rightarrow \mathbb{R}$ is bounded from below with a strict minimum in \mathbf{x}^* , which is the equilibrium state for $\mathbf{u} \equiv \mathbf{0}$. By

skew-symmetry of the interconnection matrix $\mathbf{J} = -\mathbf{J}^T$ and the definition of the collocated output, the differential energy balance

$$\dot{H}(\mathbf{x}(t)) = \mathbf{y}^T(t)\mathbf{u}(t) \quad (2)$$

holds, or in integral form,

$$H(\mathbf{x}(t_2)) - H(\mathbf{x}(t_1)) = \int_{t_1}^{t_2} \mathbf{y}^T(s)\mathbf{u}(s) ds, \quad \forall t_1 \leq t_2, \quad (3)$$

which shows passivity (see e. g. [12]) of the state representation (1). The energy balance is a *structural* or *geometric* property, i. e. it holds independently of $H(\mathbf{x})$. *Flow* and *effort* vectors are defined as

$$\mathbf{f}(t) := -\dot{\mathbf{x}}(t), \quad \mathbf{e}(t) := \nabla H(\mathbf{x}(t)). \quad (4)$$

Because of $\dot{H} = (\nabla H)^T \dot{\mathbf{x}} = -\mathbf{e}^T \mathbf{f}$, they represent *power-conjugated, dual* variables. The differential energy balance (2) can be written as the power balance equation on the *bond space* $\mathcal{F} \times \mathcal{E}$, with $\mathcal{F} = \mathbb{R}^n \times \mathbb{R}^m \ni (\mathbf{f}, \mathbf{y})$ and $\mathcal{E} = \mathbb{R}^n \times \mathbb{R}^m \ni (\mathbf{e}, \mathbf{u})$:

$$\mathbf{e}^T(t)\mathbf{f}(t) + \mathbf{y}^T(t)\mathbf{u}(t) = 0. \quad (5)$$

By

$$-\mathbf{f}(t) = \mathbf{J}(\mathbf{x}(t))\mathbf{e}(t) + \mathbf{G}(\mathbf{x}(t))\mathbf{u}(t) \quad (6a)$$

$$\mathbf{y}(t) = \mathbf{G}^T(\mathbf{x}(t))\mathbf{e}(t), \quad (6b)$$

the bond variables are constrained to a subspace (i. e. the graph of the skew-symmetric map defined in (6)), on which in particular (5) holds. This subspace is called a *Dirac structure*. For more details on Dirac structures and PH systems, see e. g. [12], Chapter 6.

3. Discrete-time PH systems based on collocation

We define the class of *discrete-time PH systems*, which arise from a *discrete-time Dirac structure*. The latter is obtained by applying the collocation method to the class of PH systems (1) and by defining in an appropriate manner *discrete flow and effort vectors* for every sampling interval. Special attention is paid on the discretization of the energy balance (3). For a *consistent* discrete-time approximation of the PH system (1), both the *supplied energy* (right hand side of (3)) and the *stored energy* (left hand side of (3)) must be approximated with the same order.

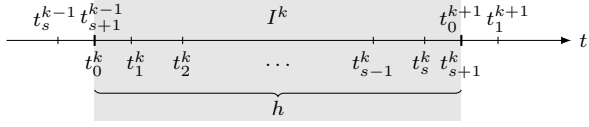


Figure 1: Sampling interval I^k with interior collocation points $t_i^k = t_0^k + c_i h$, $i = 1, \dots, s$.

3.1. Collocation method

We consider equidistant sampling intervals $I^k = [t_0^k, t_{s+1}^k] = [(k-1)h, kh]$, $k \in \mathbb{N}$ for the time t with $t_{s+1}^k = t_0^k + h$, see Fig. 1. With $t = ((k-1) + \tau)h$, the sampling intervals are parametrized by the normalized time $\tau \in [0, 1]$. The polynomial approximations of the system variables will be denoted with a tilde. As described in Section II.1.2 of [2], the numerical approximation of the solution $\mathbf{x}(t)$ of (1) is given by the vector $\tilde{\mathbf{x}}(t) \in \mathbb{R}^n$ of *collocation polynomials* of degree s . Assume first the initial value $\mathbf{x}_0^k := \tilde{\mathbf{x}}(t_0^k) = \mathbf{x}(t_0^k)$ to be known. The continuous numerical solution $\tilde{\mathbf{x}}(t)$ is then the vector of polynomials whose time derivative matches the right hand side of (1a) in the s collocation points $t_i^k := t_0^k + c_i h$ with $0 \leq c_i \leq 1$:

$$\begin{aligned} \dot{\tilde{\mathbf{x}}}(t_i^k) &= -\mathbf{f}_i^k, & i &= 1, \dots, s, \\ -\mathbf{f}_i^k &= (\mathbf{J}(\mathbf{x})\nabla H(\mathbf{x}))|_{\mathbf{x}=\tilde{\mathbf{x}}(t_i^k)} + \mathbf{G}(\tilde{\mathbf{x}}(t_i^k))\mathbf{u}(t_i^k). \end{aligned} \quad (7)$$

Notation: Arguments in *latin* letters (t or s under the integral), refer to time functions evaluated on I^k . *Greek* letters (τ or σ) refer to the same function, mapped to the normalized interval $[0, 1]$.

3.2. Approximation of flow and state variables

Based on $\mathbf{f}_i^k \in \mathbb{R}^n$, $i = 1, \dots, s$, according to (7), the interpolation formula

$$\dot{\tilde{\mathbf{x}}}(t_0^k + \tau h) =: -\tilde{\mathbf{f}}(t_0^k + \tau h) = -\sum_{i=1}^s \mathbf{f}_i^k \ell_i(\tau), \quad (8)$$

with ℓ_i the i -th Lagrange interpolation polynomial

$$\ell_i(\tau) = \prod_{\substack{j=1 \\ j \neq i}}^s \frac{\tau - c_j}{c_i - c_j}, \quad \tau \in [0, 1], \quad (9)$$

gives a polynomial approximation of $\dot{\tilde{\mathbf{x}}}(t)$ on I^k . The flow coordinates are merged in the *discrete-time flow vector*

$$\mathbf{f}^k := [(\mathbf{f}_1^k)^T \quad \dots \quad (\mathbf{f}_s^k)^T]^T \in \mathbb{R}^{sn}, \quad (10)$$

based on which the numerical solution $\tilde{\mathbf{x}}(t_0^k + \tau h)$, $\tau \in [0, 1]$ is obtained by integration of (8):

$$\tilde{\mathbf{x}}(t_0^k + \tau h) = \tilde{\mathbf{x}}(t_0^k) - h \sum_{j=1}^s \left(\mathbf{f}_j^k \int_0^\tau \ell_j(\sigma) d\sigma \right). \quad (11)$$

The values $\mathbf{x}_i^k := \tilde{\mathbf{x}}(t_i^k)$ of the numerical solution inside and at the end of the interval I^k are then computed as

$$\mathbf{x}_i^k = \mathbf{x}_0^k - h \sum_{j=1}^s a_{ij} \mathbf{f}_j^k, \quad i = 1, \dots, s, \quad (12)$$

$$\mathbf{x}_{s+1}^k = \mathbf{x}_0^k - h \sum_{j=1}^s b_j \mathbf{f}_j^k, \quad (13)$$

with² ($i, j = 1, \dots, s$)

$$a_{ij} = \int_0^{c_i} \ell_j(\sigma) d\sigma, \quad b_j = \int_0^1 \ell_j(\sigma) d\sigma. \quad (14)$$

In *continuous* collocation methods, the numerical solution at the start $t_0^{k+1} = t_{s+1}^k$ of the subsequent interval is initialized by $\mathbf{x}_0^{k+1} = \mathbf{x}_{s+1}^k$.

3.3. Effort approximation and discrete structure equation

The definition of the discrete flow coordinates $\mathbf{f}_1^k, \dots, \mathbf{f}_s^k$ in (7) requires to evaluate the effort vector $\nabla H(\mathbf{x}(t))$, the input $\mathbf{u}(t)$ and the interconnection and input matrices $\mathbf{J}(\mathbf{x}(t))$, $\mathbf{G}(\mathbf{x}(t))$ in the flow collocation points c_i ,

$$\mathbf{e}_i^k := \nabla H(\mathbf{x})|_{\mathbf{x}^k}, \quad \mathbf{u}_i^k := \mathbf{u}(t_0^k + c_i h), \quad (15)$$

and

$$\mathbf{J}_i^k := \mathbf{J}(\mathbf{x}_i^k), \quad \mathbf{G}_i^k := \mathbf{G}(\mathbf{x}_i^k) \quad (16)$$

for $i = 1, \dots, s$. The discrete-time counterpart of (6a) is then

$$-\mathbf{f}_i^k = \mathbf{J}_i^k \mathbf{e}_i^k + \mathbf{G}_i^k \mathbf{u}_i^k, \quad (17)$$

with $\mathbf{J}_i^k = -(\mathbf{J}_i^k)^T$. With $\mathbf{e}_i^k \in \mathbb{R}^n$ and $\mathbf{u}_i^k \in \mathbb{R}^m$ the *discrete effort* and *discrete input coordinates* according to (15), the polynomial approximations of the effort and the input vector are

$$\tilde{\mathbf{e}}(t_0^k + \tau h) = \sum_{i=1}^s \mathbf{e}_i^k \ell_i(\tau), \quad \tilde{\mathbf{u}}(t_0^k + \tau h) = \sum_{i=1}^s \mathbf{u}_i^k \ell_i(\tau). \quad (18)$$

²These values are, together with c_i , the coefficients of the Butcher table for the Runge-Kutta (RK) interpretation of the collocation method, see [2], Theorem II.1.4.

In accordance with the approximate flows, we define the *discrete-time effort vector* and the *discrete-time input vector*

$$\mathbf{e}^k = [(\mathbf{e}_1^k)^T \ \dots \ (\mathbf{e}_s^k)^T]^T \in \mathbb{R}^{sn}, \quad (19)$$

$$\mathbf{u}^k = [(\mathbf{u}_1^k)^T \ \dots \ (\mathbf{u}_s^k)^T]^T \in \mathbb{R}^{sm}. \quad (20)$$

Defining the block-diagonal matrices

$$\begin{aligned} \mathbf{J}^k &= -(\mathbf{J}^k)^T = \text{blockdiag}(\mathbf{J}_1^k, \dots, \mathbf{J}_s^k), \\ \mathbf{G}^k &= \text{blockdiag}(\mathbf{G}_1^k, \dots, \mathbf{G}_s^k), \end{aligned} \quad (21)$$

the *structure equation* (17) on the sampling interval I^k can be rewritten as

$$-\mathbf{f}^k = \mathbf{J}^k \mathbf{e}^k + \mathbf{G}^k \mathbf{u}^k. \quad (22)$$

Remark 1. Defining the discrete effort and input coordinates based on *different* collocation points d_1, \dots, d_r is also conceivable. In this case, the terms of the right hand side of (17) must be replaced by interpolations between the effort collocation points according to (18). In this paper, we restrict ourselves to *identical* collocation points for the flow and effort variables, and to the explicit representation of the resulting Dirac structure and PH system.

3.4. Discrete-time supplied energy

Since the instantaneous (local) power balance results trivially from the equations of the Dirac structure, we seek to express a discrete-time counterpart of the integral energy balance equation (3) on the time interval I^k . To this end, we integrate the polynomial approximation of instantaneous power $-\tilde{\mathbf{e}}^T(t_0^k + \tau h)\tilde{\mathbf{f}}(t_0^k + \tau h)$ over the normalized time interval $[0, 1]$, and obtain an *approximation of supplied energy* on the sampling interval I^k

$$\Delta \tilde{H}^k := -h \int_0^1 \tilde{\mathbf{e}}^T(t_0^k + \sigma h)\tilde{\mathbf{f}}(t_0^k + \sigma h) d\sigma. \quad (23)$$

Substituting the definitions (8) and (18) of the polynomial flow and effort approximations, we obtain the bilinear form

$$\Delta \tilde{H}^k = -h(\mathbf{e}^k)^T \mathbf{M} \mathbf{f}^k \quad (24)$$

with the symmetric matrix $\mathbf{M} = \mathbf{M}^T \in \mathbb{R}^{sn \times sn}$,

$$\mathbf{M} = \begin{bmatrix} m_{11} & \dots & m_{1s} \\ \vdots & \ddots & \vdots \\ m_{s1} & \dots & m_{ss} \end{bmatrix} \otimes \mathbf{I}_n, \quad m_{ij} = \int_0^1 \ell_i(\sigma)\ell_j(\sigma) d\sigma, \quad (25)$$

where $m_{ij} = m_{ji}$ and \otimes denotes the Kronecker product.

Remark 2. We can understand the term $\mathbf{M}\mathbf{e}^k$ as a generalization of the *discrete gradient* and $-h\mathbf{f}^k$ as a vector generalizing the increment of the numerical solution in the integration step.

3.5. Discrete-time Dirac structure

We provide conditions under which the polynomial approximation of the power variables leads to the definition of a discrete-time Dirac structure. Substituting the relation (22) in the right hand side of the discrete energy balance (24), we obtain

$$-h(\mathbf{e}^k)^T \mathbf{M} \mathbf{f}^k = h(\mathbf{e}^k)^T \mathbf{M} \mathbf{J}^k \mathbf{e}^k + h(\mathbf{e}^k)^T \mathbf{M} \mathbf{G}^k \mathbf{u}^k. \quad (26)$$

At this stage, we want to recover a discrete-time equivalent of the structural power balance (5). To this end, the first term on the right hand side must vanish: $h(\mathbf{e}^k)^T \mathbf{M} \mathbf{J}^k \mathbf{e}^k \stackrel{!}{=} 0$ for all $\mathbf{e}^k \in \mathbb{R}^{sn}$, or written element-wise (recall $m_{ij} = m_{ji}$),

$$h \sum_{i=1}^s \sum_{j=1}^s (\mathbf{e}_i^k)^T m_{ij} \mathbf{J}_j^k \mathbf{e}_j^k \stackrel{!}{=} 0. \quad (27)$$

By skew-symmetry of \mathbf{J}_j^k , we have $(\mathbf{e}_j^k)^T m_{jj} \mathbf{J}_j^k \mathbf{e}_j^k = 0$ for all $j = 1, \dots, s$. The remaining elements of the sum cancel to zero, if $(\mathbf{e}_i^k)^T m_{ij} \mathbf{J}_j^k \mathbf{e}_j^k = -(\mathbf{e}_j^k)^T m_{ji} \mathbf{J}_i^k \mathbf{e}_i^k$ holds for all $i \neq j$. With $(\mathbf{e}_i^k)^T m_{ij} \mathbf{J}_j^k \mathbf{e}_j^k = -((\mathbf{e}_i^k)^T m_{ij} (\mathbf{J}_j^k)^T \mathbf{e}_j^k)^T = -(\mathbf{e}_j^k)^T m_{ji} \mathbf{J}_i^k \mathbf{e}_i^k$, the requirement translates to

$$(\mathbf{e}_j^k)^T m_{ji} \mathbf{J}_i^k \mathbf{e}_i^k = (\mathbf{e}_i^k)^T m_{ij} \mathbf{J}_j^k \mathbf{e}_j^k \quad \forall i \neq j, \quad (28)$$

which is true if either of the following conditions holds.

$$(C1) \quad m_{ij} = 0 \text{ for all } i \neq j,$$

$$(C2) \quad \mathbf{J}_i^k = \mathbf{J}_j^k = \text{const. for all } i, j = 1, \dots, s.$$

While (C1) is an orthogonality condition on the choice of the approximation basis in the *discretization method*, the constant interconnection structure according to (C2) is a *system property*³.

In both cases (C1) or (C2), the discrete energy balance (26) boils down to

$$h(\mathbf{e}^k)^T \mathbf{M} \mathbf{f}^k + h(\mathbf{e}^k)^T \mathbf{M} \mathbf{G}^k \mathbf{u}^k = 0. \quad (29)$$

³Darboux-Lie theorem states that every Poisson system can be transformed locally to a canonical Hamiltonian system with a constant skew-symmetric matrix ([2], Section VII.3). Condition (C2) is then satisfied if the original PH systems is expressed in terms of these canonical local coordinates.

The definition of a *discrete-time output vector*

$$\mathbf{y}^k := (\mathbf{G}^k)^T \mathbf{M} \mathbf{e}^k \quad (30)$$

yields (using $\mathbf{M} = \mathbf{M}^T$)

$$h(\mathbf{M} \mathbf{e}^k)^T \mathbf{f}^k + h(\mathbf{y}^k)^T \mathbf{u}^k = 0, \quad (31)$$

which represents a *structural balance equation* for the supplied energy in I^k (or average supplied power, if divided by h). We are ready to define the discrete-time Dirac structure, which is based on the polynomial approximation of the power variables.

Theorem 1 (Discrete-time Dirac structure). *Given the s collocation points $0 \leq c_i \leq 1$, $i = 1, \dots, s$. The system of equations (22), (30), i. e.*

$$\begin{aligned} -\mathbf{f}^k &= \mathbf{J}^k \mathbf{e}^k + \mathbf{G}^k \mathbf{u}^k \\ \mathbf{y}^k &= (\mathbf{G}^k)^T \mathbf{M} \mathbf{e}^k, \end{aligned} \quad (32)$$

with discrete flow, effort and input vectors \mathbf{f}^k , \mathbf{e}^k , \mathbf{u}^k according to (10), (19), (20), the block matrices $\mathbf{J}^k = -(\mathbf{J}^k)^T$, \mathbf{G}^k according to (21), and the symmetric block matrix $\mathbf{M} = \mathbf{M}^T$ according to (25), represents a discrete-time Dirac structure on the time interval $I^k = [(k-1)h, kh]$, if either condition (C1) or (C2) is satisfied.

Proof. Rewrite (32) in kernel representation

$$\mathbf{F} \begin{bmatrix} \mathbf{f}^k \\ \mathbf{y}^k \end{bmatrix} + \mathbf{E} \begin{bmatrix} \mathbf{M} \mathbf{e}^k \\ \mathbf{u}^k \end{bmatrix} = \mathbf{0} \quad (33)$$

with

$$\mathbf{F} = \mathbf{I}_{s(n+m)}, \quad \mathbf{E} = \begin{bmatrix} \mathbf{J}^k \mathbf{M}^{-1} & \mathbf{G}^k \\ -(\mathbf{G}^k)^T & \mathbf{0} \end{bmatrix}. \quad (34)$$

According to [12], Prop. 6.6.6, the subspace of discrete bond variables $(\mathbf{f}^k, \mathbf{M} \mathbf{e}^k)$ and $(\mathbf{y}^k, \mathbf{u}^k)$ on which (33) holds, is a Dirac structure, if (i) $\mathbf{E} \mathbf{F}^T + \mathbf{F} \mathbf{E}^T = \mathbf{0}$ and (ii) the matrix $[\mathbf{F} \ \mathbf{E}]$ has full row rank $s(n+m)$. The latter is obvious from $\mathbf{F} = \mathbf{I}_{s(n+m)}$. Condition (i) is satisfied if and only if $\mathbf{J}^k \mathbf{M}^{-1}$ or, equivalently, $\mathbf{M} \mathbf{J}^k$ is skew-symmetric. As shown above, the latter holds if the continuous-time system has a constant interconnection matrix (C2) or the choice of collocation points guarantees (C1). \square

3.6. Discrete-time port-Hamiltonian system

The discrete-time Dirac structure is now complemented by discrete-time dynamics and constitutive equations.

Definition 1 (Discrete-time PH system). Equations (32), together with the *s-stage discrete dynamics*

$$\mathbf{x}_0^k = \mathbf{x}_{s+1}^{k-1}, \quad (35a)$$

$$\mathbf{x}_i^k = \mathbf{x}_0^k - h \sum_{j=1}^s a_{ij} \mathbf{f}_j^k, \quad i = 1, \dots, s, \quad (35b)$$

$$\mathbf{x}_{s+1}^k = \mathbf{x}_0^k - h \sum_{j=1}^s b_j \mathbf{f}_j^k, \quad (35c)$$

with Runge-Kutta coefficients a_{ij} and b_j according to (14) and the *discrete constitutive equations*

$$\mathbf{e}_i^k = \nabla H(\mathbf{x})|_{\mathbf{x}=\mathbf{x}_i^k}, \quad i = 1, \dots, s, \quad (36)$$

define a *discrete-time PH system*. Using (24) and (31), the approximation of energy supplied to the storage elements on the sampling interval $I^k = [(k-1)h, kh]$ is given by

$$\Delta \tilde{H}^k = h(\mathbf{y}^k)^T \mathbf{u}^k. \quad (37)$$

Remark 3. Equations (35b) and (35c) can be written in more compact form using the Kronecker product

$$\mathbf{x}_i^k = \mathbf{x}_0^k - h(\mathbf{a}_i^T \otimes \mathbf{I}_n) \mathbf{f}^k, \quad i = 1, \dots, s, \quad (38a)$$

$$\mathbf{x}_{s+1}^k = \mathbf{x}_0^k - h(\mathbf{b}^T \otimes \mathbf{I}_n) \mathbf{f}^k, \quad (38b)$$

with $\mathbf{a}_i^T = [a_{i1} \ \dots \ a_{is}]$, $\mathbf{b}^T = [b_1 \ \dots \ b_s]$.

Remark 4. The *structure* of the discrete-time PH models is independent of the sampling time h , which, however, determines the approximation quality.

3.7. Stored energy approximation and discrete energy balance

Equation (37) represents an approximation of the *supplied energy* flow through the port $(\mathbf{u}(t), \mathbf{y}(t))$ based on the polynomial approximation of flows and efforts. On the other hand, the difference

$$\Delta \bar{H}^k = H(\mathbf{x}_{s+1}^k) - H(\mathbf{x}_0^k) \quad (39)$$

expresses the increment of *stored energy* based on a numerical integration scheme (35), as opposed to the exact increment

$$\Delta H^k = H(\mathbf{x}(t_0^k + h)) - H(\mathbf{x}(t_0^k)). \quad (40)$$

Definition 2. If under a given numerical integration scheme of order p , the increment of stored energy satisfies

$$\Delta \bar{H}^k = h(\mathbf{y}^k)^T \mathbf{u}^k + o(h^p), \quad (41)$$

we call (41) a *discrete energy balance*, which is *consistent* with the discretization scheme. If

$$\Delta \bar{H}^k = h(\mathbf{y}^k)^T \mathbf{u}^k \quad (42)$$

we call the energy balance *exact*.

Remark 5. In Definition III.2 of [9], the latter case is simply called “discrete energy balance”. As (42) only holds under additional conditions, like constant structure and quadratic energy matrix, and for example under the implicit midpoint rule (see [6], Section III.B and [9], Section III.E), we add “exact” to distinguish this particular case of a discrete energy balance.

To show the consistency of a discrete energy balance, we will show that the local approximation errors of both $\Delta \bar{H}^k$ and $\Delta \tilde{H}^k$, compared with the exact increment ΔH^k with $\mathbf{x}_0^k = \mathbf{x}(t_0^k)$, have order $o(h^p)$. To perform this analysis, we restrict ourselves to quadratic energies of the form

$$H(\mathbf{x}) = \frac{1}{2} \mathbf{x}^T \mathbf{Q} \mathbf{x}, \quad \mathbf{Q} = \mathbf{Q}^T > 0. \quad (43)$$

Theorem 2 (Local error of stored energy). *For a quadratic energy (43), the local energy error*

$$\Delta \bar{H}^k - \Delta H^k, \quad \mathbf{x}_0^k = \mathbf{x}(t_0^k), \quad (44)$$

is consistent with the numerical integration scheme, i. e. it has order $o(h^p)$.

Proof. For an integration scheme of order p , the local approximation error or consistency error (set $\mathbf{x}_0^k = \tilde{\mathbf{x}}(t_0^k) = \mathbf{x}(t_0^k)$) has order $o(h^p)$: $\|\tilde{\mathbf{x}}(t_0^k + h) - \mathbf{x}(t_0^k + h)\| \leq C_1 h^{p+1}$, $C_1 > 0$. By the equivalence of norms, this holds accordingly for the energy norm $\|\mathbf{x}\|_Q := \sqrt{\frac{1}{2} \mathbf{x}^T \mathbf{Q} \mathbf{x}}$, with a different constant $C_2 > 0$: $\|\tilde{\mathbf{x}}(t_0^k + h) - \mathbf{x}(t_0^k + h)\|_Q \leq C_2 h^{p+1}$. For the error in the supplied energy, the following estimate can be given ($t_{s+1}^k = t_0^k + h$), where the triangle inequality is used between third and fourth line ($\mathbf{x}_{s+1}^k = \tilde{\mathbf{x}}(t_{s+1}^k)$):

$$\begin{aligned} |\Delta \bar{H}^k - \Delta H^k| &= \left| \|\mathbf{x}_{s+1}^k\|_Q^2 - \|\mathbf{x}(t_{s+1}^k)\|_Q^2 \right| \\ &= \left| \left(\|\mathbf{x}_{s+1}^k\|_Q + \|\mathbf{x}(t_{s+1}^k)\|_Q \right) \cdot \left(\|\mathbf{x}_{s+1}^k\|_Q - \|\mathbf{x}(t_{s+1}^k)\|_Q \right) \right| \\ &\leq 2 \max \left(\|\mathbf{x}_{s+1}^k\|_Q, \|\mathbf{x}(t_{s+1}^k)\|_Q \right) \cdot \left| \|\mathbf{x}_{s+1}^k\|_Q - \|\mathbf{x}(t_{s+1}^k)\|_Q \right| \\ &\leq 2 \max \left(\|\mathbf{x}_{s+1}^k\|_Q, \|\mathbf{x}(t_{s+1}^k)\|_Q \right) \cdot \left\| \mathbf{x}_{s+1}^k - \mathbf{x}(t_{s+1}^k) \right\|_Q \\ &\leq C_3 h^{p+1} \end{aligned} \quad (45)$$

with $C_3 = 2 \max \left(\|\mathbf{x}_{s+1}^k\|_Q, \|\mathbf{x}(t_{s+1}^k)\|_Q \right) C_2$. \square

In the following section, we will discuss Gauss-Legendre collocation and the Lobatto IIIA/IIIB pairs as examples for symplectic integration schemes. In the former case, we will prove that $\Delta \bar{H}^k = \Delta \tilde{H}^k$ holds for quadratic energies. In the latter case, we will show that $\Delta \tilde{H}^k$ approximates the energy increment ΔH^k with an error of identical order as $\Delta \bar{H}^k$, and consequently the discrete energy balance (41) holds.

4. Examples and analysis of energy errors

The degrees of freedom to define a discrete-time PH system according to Definition 1 are (i) the set of collocation points $\{c_1, \dots, c_s\}$ and (ii) the concrete coefficients a_{ij} and weights b_j of the RK integration scheme (35). In this Section, we consider two classes of s -stage symplectic integration schemes: Gauss-Legendre collocation and the Lobatto IIIA/IIIB pairs for partitioned systems. In both cases, we analyze the error of the supplied energy approximation $\Delta \tilde{H}^k$ for quadratic energies and its relation to $\Delta \bar{H}^k$ in the light of Definition 2.

4.1. Gauss-Legendre collocation

To define a discrete-time Dirac structure for cases with non-constant interconnection matrices, condition (C1) must be satisfied by the choice of collocation points. To have $m_{ij} = m_{ji} = 0$ for $i \neq j$, with m_{ij} defined in (25), the interpolation polynomials $\{\ell_1(\tau), \dots, \ell_s(\tau)\}$ must form a system of *orthogonal* functions. This is the case, if we take the collocation points c_1, \dots, c_s as the zeros of the shifted Legendre polynomials⁴

$$\frac{d^s}{d\tau^s} (\tau^s (\tau - 1)^s) \quad (46)$$

in normalized time $\tau \in [0, 1]$. With the resulting interpolation polynomials, the diagonal elements of \mathbf{M} ,

$$m_{ii} = \int_0^1 \ell_i^2(\sigma) d\sigma = \int_0^1 \ell_i(\sigma) d\sigma = b_i, \quad (47)$$

equal the weights b_i in the Gauss-Legendre quadrature formula

$$\int_0^1 f(\sigma) d\sigma \approx \sum_{i=1}^s b_i f(c_i). \quad (48)$$

⁴See [2], Section II.1.3.

This quadrature formula is *exact* for polynomials $f(\tau)$ on $[0, 1]$ up to order $2s - 1$. With $2s$ the order of the quadrature formula, the approximation error of the integral

$$\int_{t_0}^{t_0+h} f(s) ds = h \int_0^1 f(t_0+h\sigma) d\sigma \approx h \sum_{i=1}^s b_i f(t_0+hc_i) \quad (49)$$

is of order $\mathcal{O}(h^{2s+1})$. The coefficients a_{ij} of the unique implicit Runge-Kutta (RK) method⁵ of order $p = 2s$ can be computed as given in (14).

We now determine the conditions on the parameters of the integration scheme under which $\Delta\bar{H}^k = \Delta\tilde{H}^k$. Substituting (35c) in (39) for a quadratic energy, we have

$$\begin{aligned} \Delta\bar{H}^k &= -h(\mathbf{x}_0^k)^T \mathbf{Q} \sum_{j=1}^s b_j \mathbf{f}_j^k \\ &\quad + \frac{1}{2} h^2 \left(\sum_{j=1}^s b_j \mathbf{f}_j^k \right)^T \mathbf{Q} \sum_{j=1}^s b_j \mathbf{f}_j^k. \end{aligned} \quad (50)$$

On the other hand, with $b_j = m_{jj}$, $\mathbf{e}_j^k = \mathbf{Q}\mathbf{x}_j^k$ and (35c), Equation (24) becomes

$$\begin{aligned} \Delta\tilde{H}^k &= -h \sum_{j=1}^s (\mathbf{e}_j^k)^T m_{jj} \mathbf{f}_j^k \\ &= -h \sum_{j=1}^s (\mathbf{x}_0^k - h \sum_{l=1}^s a_{jl} \mathbf{f}_l^k)^T \mathbf{Q} b_j \mathbf{f}_j^k \\ &= -h(\mathbf{x}_0^k)^T \mathbf{Q} \sum_{j=1}^s b_j \mathbf{f}_j^k + h^2 \sum_{j=1}^s \left(\left(\sum_{l=1}^s a_{jl} \mathbf{f}_l^k \right)^T \mathbf{Q} b_j \mathbf{f}_j^k \right). \end{aligned} \quad (51)$$

The first terms in (50) and (51) are identical. By matching the coefficients in front of $h^2(\mathbf{f}_l^k)^T \mathbf{Q} b_j \mathbf{f}_j^k$ in the second term, one obtains the conditions

$$a_{ii} = \frac{1}{2} b_i, \quad a_{ij} b_i + a_{ji} b_j = b_i b_j \quad (52)$$

for $i, j = 1, \dots, s$, under which $\Delta\bar{H}^k$ and $\Delta\tilde{H}^k$ coincide.

Theorem 3. *The s -stage Gauss-Legendre collocation methods, applied to PH systems with quadratic energy, are the only numerical integration schemes, which yield an exact discrete energy balance (42).*

⁵See the Butcher tables in [2], Section II.1.3.

Proof. Equation (52) is only satisfied for Gauss-Legendre collocation, see [2], Section IV.2.1, Theorem 2.2 and the paragraph below the proof⁶. If (52) is true, $\Delta\bar{H}^k = \Delta\tilde{H}^k$ holds, and (42) follows from (37). \square

Remark 6. Gauss-Legendre collocation with $s = 1$ leads to the implicit midpoint rule, which is shown in [6] to satisfy an exact discrete energy balance. Theorem 3 shows that this is not the only choice for structure-preserving time discretization of PH systems with exact energy balance.

4.2. Lobatto IIIA/IIIB pairs

Partitioned collocation methods, such as Lobatto pairs are used for separable Hamiltonian systems. We consider in this study the linear PH system of simple mechanical type⁷ with $\mathbf{q}, \mathbf{p} \in \mathbb{R}^n$, $\mathbf{u} \in \mathbb{R}^m$,

$$\begin{aligned} \begin{bmatrix} \dot{\mathbf{q}}(t) \\ \dot{\mathbf{p}}(t) \end{bmatrix} &= \begin{bmatrix} \mathbf{0} & \mathbf{I} \\ -\mathbf{I} & \mathbf{0} \end{bmatrix} \begin{bmatrix} \mathbf{Q}\mathbf{q}(t) \\ \mathbf{P}\mathbf{p}(t) \end{bmatrix} + \begin{bmatrix} \mathbf{0} \\ \mathbf{G} \end{bmatrix} \mathbf{u}(t) \\ \mathbf{y}(t) &= \begin{bmatrix} \mathbf{0} & \mathbf{G}^T \end{bmatrix} \begin{bmatrix} \mathbf{Q}\mathbf{q}(t) \\ \mathbf{P}\mathbf{p}(t) \end{bmatrix}. \end{aligned} \quad (53)$$

The discrete-time structure equations can be expressed as

$$\begin{bmatrix} -\mathbf{f}_q^k \\ -\mathbf{f}_p^k \end{bmatrix} = \begin{bmatrix} \mathbf{0} & \mathbf{I}_{sn} \\ -\mathbf{I}_{sn} & \mathbf{0} \end{bmatrix} \begin{bmatrix} \mathbf{e}_q^k \\ \mathbf{e}_p^k \end{bmatrix} + \begin{bmatrix} \mathbf{0} \\ \mathbf{G}^k \end{bmatrix} \mathbf{u}^k. \quad (54)$$

The elements of the effort and input vectors $\mathbf{e}_q^k, \mathbf{e}_p^k \in \mathbb{R}^{sn}$, $\mathbf{u}^k \in \mathbb{R}^{sm}$ are

$$\mathbf{e}_{q,i}^k = \mathbf{Q}\mathbf{q}_i^k, \quad \mathbf{e}_{p,i}^k = \mathbf{P}\mathbf{p}_i^k, \quad \mathbf{u}_i^k = \mathbf{u}(t_0^k + c_i h). \quad (55)$$

The partitioned integration scheme, which consists of two RK methods (coefficients a_{ij} , \hat{a}_{ij} , $b_j = \hat{b}_j$, $c_i = \hat{c}_i$, $i, j = 1, \dots, s$), each applied to one set of differential equations, can be written ($i = 1, \dots, s$)

$$\mathbf{q}_0^k = \mathbf{q}_{s+1}^{k-1}, \quad \mathbf{p}_0^k = \mathbf{p}_{s+1}^{k-1}, \quad (56a)$$

$$\mathbf{q}_i^k = \mathbf{q}_0^k - h \sum_{j=1}^s a_{ij} \mathbf{f}_{q,j}^k, \quad \mathbf{p}_i^k = \mathbf{p}_0^k - h \sum_{j=1}^s \hat{a}_{ij} \mathbf{f}_{p,j}^k, \quad (56b)$$

$$\mathbf{q}_{s+1}^k = \mathbf{q}_0^k - h \sum_{j=1}^s b_j \mathbf{f}_{q,j}^k, \quad \mathbf{p}_{s+1}^k = \mathbf{p}_0^k - h \sum_{j=1}^s \hat{b}_j \mathbf{f}_{p,j}^k, \quad (56c)$$

⁶The criterion (52) characterizes numerical integration methods that conserve quadratic invariants. “[A]mong all collocation and discontinuous collocation methods [...] only the Gauss methods satisfy this criterion [...]”

⁷ $\mathbf{Q} = \mathbf{K}$ denotes the stiffness matrix, $\mathbf{P} = \mathbf{M}^{-1}$ the inverse mass matrix.

with $\mathbf{f}_{q,j}^k = -\mathbf{e}_{p,j}^k$, $\mathbf{f}_{p,j}^k = \mathbf{e}_{q,j}^k - \mathbf{G}^k \mathbf{u}_j^k$, $j = 1, \dots, s$.

In contrast to Gauss-Legendre collocation, the expression for the increment of a quadratic Hamiltonian per sampling interval

$$\begin{aligned} \Delta \bar{H}^k &= \frac{1}{2}(\mathbf{q}_{s+1}^k)^T \mathbf{Q} \mathbf{q}_{s+1}^k - \frac{1}{2}(q_0^k)^T \mathbf{Q} \mathbf{q}_0^k \\ &\quad + \frac{1}{2}(\mathbf{p}_{s+1}^k)^T \mathbf{P} \mathbf{p}_{s+1}^k - \frac{1}{2}(\mathbf{p}_0^k)^T \mathbf{P} \mathbf{p}_0^k \end{aligned} \quad (57)$$

does *not* coincide with the approximate supplied energy

$$\begin{aligned} \Delta \tilde{H}^k &= - \int_{t_0^k}^{t_0^k+h} \tilde{\mathbf{e}}_q^T(s) \tilde{\mathbf{f}}_q(s) + \tilde{\mathbf{e}}_p^T(s) \tilde{\mathbf{f}}_p(s) ds \\ &= -h(\mathbf{e}_q^k)^T \mathbf{M} \mathbf{f}_q^k - h(\mathbf{e}_p^k)^T \mathbf{M} \mathbf{f}_p^k, \end{aligned} \quad (58)$$

where \mathbf{M} is given by (25).

We restrict our attention to the 3-stage Lobatto pair⁸ with collocation points $c_1 = 0$, $c_2 = \frac{1}{2}$, $c_3 = 1$, in which case the matrix \mathbf{M} is

$$\mathbf{M} = \begin{bmatrix} \frac{2}{15} & \frac{1}{15} & -\frac{1}{30} \\ \frac{1}{15} & \frac{1}{15} & \frac{1}{15} \\ -\frac{1}{30} & \frac{1}{15} & \frac{1}{15} \end{bmatrix} \otimes \mathbf{I}_n. \quad (59)$$

Theorem 4. *For the 3-stage Lobatto pair, applied to the partitioned linear PH system (53), the error between $\Delta \tilde{H}^k$ and $\Delta \bar{H}^k$, and consequently the error between $\Delta \tilde{H}^k$ and ΔH^k has order $o(h^{2s-2}) = o(h^4)$.*

Proof. First notice that the local energy error $\Delta \bar{H}^k - \Delta H^k$ is of order $o(h^p)$ with $p = 2s - 2$ the order of the Lobatto pair, see Theorem 1. To prove that the error $\Delta \tilde{H}^k - \Delta \bar{H}^k$ has the same order, the expressions in (57) and (58) are subtracted, under substitution of the efforts and states in the i -th stage according to (55) and (56b). We replace the terms $\mathbf{f}_{q,1}^k$, $\mathbf{f}_{q,3}^k$ and $\mathbf{f}_{p,1}^k$, $\mathbf{f}_{p,3}^k$ by their Taylor expansions

$$\begin{aligned} \mathbf{f}_{q,1}^k &= \mathbf{f}_{q,2}^k - \dot{\mathbf{f}}_{q,2}^k \frac{h}{2} + \mathbf{r}_1 h^2, & \mathbf{f}_{q,3}^k &= \mathbf{f}_{q,2}^k + \dot{\mathbf{f}}_{q,2}^k \frac{h}{2} + \mathbf{r}_2 h^2 \\ \mathbf{f}_{p,1}^k &= \mathbf{f}_{p,2}^k - \dot{\mathbf{f}}_{p,2}^k \frac{h}{2} + \mathbf{r}_3 h^2, & \mathbf{f}_{p,3}^k &= \mathbf{f}_{p,2}^k + \dot{\mathbf{f}}_{p,2}^k \frac{h}{2} + \mathbf{r}_4 h^2, \end{aligned} \quad (60)$$

where $\dot{\mathbf{f}}_{q,2}^k = \frac{d}{dt} \tilde{\mathbf{f}}_q(t_2^k)$ and $\dot{\mathbf{f}}_{p,2}^k = \frac{d}{dt} \tilde{\mathbf{f}}_p(t_2^k)$ are the time derivatives of the polynomial flow approximations $\tilde{\mathbf{f}}_q$ and $\tilde{\mathbf{f}}_p$ in $t_2^k = t_0^k + \frac{h}{2}$. $\mathbf{r}_1, \dots, \mathbf{r}_4$ are residual

terms. The result is

$$\begin{aligned} \Delta \bar{H}^k - \Delta \tilde{H}^k &= F_1(\mathbf{r}_1, \dots, \mathbf{r}_4, \dot{\mathbf{f}}_{q,2}^k, \dot{\mathbf{f}}_{p,2}^k) h^5 \\ &\quad + F_2(\mathbf{r}_1, \dots, \mathbf{r}_4) h^6, \end{aligned} \quad (61)$$

where F_1 and F_2 are functions in the given arguments. This, together with the order of the error $\Delta \bar{H}^k - \Delta H^k$, proves the claim. \square

As a consequence of Theorem 4, the application of the 3-stage Lobatto pair to the partitioned PH system (53) defines a discrete-time PH system, whose discrete energy balance is consistent with the order $p = 2s - 2 = 4$ of the numerical scheme.

Theorem 4 shows exemplarily at the case $s = 3$ how to prove the identical consistency order of both local energy approximation errors. The numerical experiments in the following section give evidence that the corresponding order statement also holds for the 4-stage Lobatto pair.

5. Numerical experiments

We illustrate the quantitative statements concerning the accuracy of the energy approximations by the numerical simulation of a linear oscillator, whose solutions can be computed, and which therefore serves as a benchmark example. First, the conservative case, which has been considered throughout the paper, is studied. The accumulated errors of energy supplied through the port $(u(t), y(t))$ and stored energy are determined and illustrated for both considered families of integration schemes. In a second part, the control port is closed by constant feedback, which injects damping to the system. We show that the accuracy order of the energy approximation is maintained in the lossy case.

The considered state PH model of the lossless oscillator is given by the explicit representation of the underlying Dirac structure

$$-\mathbf{f}(t) = \mathbf{J} \mathbf{e}(t) + \mathbf{g} u(t) \quad (62a)$$

$$\mathbf{y}(t) = \mathbf{g}^T \mathbf{e}(t) \quad (62b)$$

with flow and effort vectors $\mathbf{f}, \mathbf{e} \in \mathbb{R}^2$, in- and output $u, y \in \mathbb{R}$.

$$\mathbf{J} = \begin{bmatrix} 0 & 1 \\ -1 & 0 \end{bmatrix} \quad \text{and} \quad \mathbf{g} = \begin{bmatrix} 0 \\ 1 \end{bmatrix} \quad (63)$$

denote the interconnection matrix and the input vector. The dynamics equation is $\dot{\mathbf{x}}(t) = -\mathbf{f}(t)$

⁸See the Butcher tables in [2], Section II.1.4.

with $\mathbf{x} \in \mathbb{R}^2$ the state vector. The linear constitutive equations $\mathbf{e}(t) = \mathbf{Q}\mathbf{x}(t)$ are derived from the quadratic Hamiltonian $H(\mathbf{x}) = \frac{1}{2}\mathbf{x}^T\mathbf{Q}\mathbf{x}$ with $\mathbf{Q} = \mathbf{I}$. For the lossy case, the extended output feedback

$$u(t) = -ry(t) + v(t), \quad r > 0, \quad (64)$$

with new input $v(t)$, generates the damped system's state differential equation

$$\dot{\mathbf{x}}(t) = (\mathbf{J} - \mathbf{R})\mathbf{Q}\mathbf{x}(t) + \mathbf{g}v(t), \quad \mathbf{R} = \begin{bmatrix} 0 & 0 \\ 0 & r \end{bmatrix}. \quad (65)$$

The structure equations (62) are discretized using collocation as described in the previous sections. First, Gauss-Legendre collocation with $s = 1, 2, 3$ stages is used. Then, the partitioned representation of (62) is considered for the discretization of the Dirac structure with 3- and 4-stage Lobatto pairs. Discrete-time dynamics and constitutive equations are discretized according to Definition 1, again considering the partitioned version of the state space model for the Lobatto pairs.

5.1. Energy supply and storage in the lossless case

Starting from an initial state $\mathbf{x}(0) = [q(0) \ p(0)]^T = [0 \ -1]^T$, the undamped system is excited by a pulse-shaped input

$$u(t) = \begin{cases} 0, & t < 8 \\ \sin^2\left(\frac{t-8}{10-8}\pi\right), & 8 \leq t \leq 10 \\ 0, & t > 10. \end{cases} \quad (66)$$

Figure 2 shows the exact evolutions of states, input and the quadratic energy for this test case on the interval $[0, T_{\text{end}}] = [0, 18]$. Figure 3 depicts the magnitude of relative errors

$$\tilde{\epsilon}_H := \frac{\Delta\tilde{H}_{\text{tot}} - \Delta H_{\text{tot}}}{\Delta H_{\text{tot}}}, \quad \bar{\epsilon}_H := \frac{\Delta\bar{H}_{\text{tot}} - \Delta H_{\text{tot}}}{\Delta H_{\text{tot}}} \quad (67)$$

of total supplied and stored energy over the range of step sizes $h \in [0.005, 0.5]$. $\Delta H_{\text{tot}} = \sum_{k=1}^N \Delta H^k$, $\Delta\tilde{H}_{\text{tot}} = \sum_{k=1}^N \Delta\tilde{H}^k$ and $\Delta\bar{H}_{\text{tot}} = \sum_{k=1}^N \Delta\bar{H}^k$ denote the total increment of energy and its approximations on $[0, T_{\text{end}}]$ with $N = T_{\text{end}}/h$ the number of sampling intervals. With $\Delta\bar{H}^k = \Delta H^k + c^k h^{p+1}$, where p is the order of the integration scheme, the absolute value of $\bar{\epsilon}_H$ can be bounded as follows:

$$|\bar{\epsilon}_H| = \frac{|\sum_{k=1}^N c^k h^{p+1}|}{|\sum_{k=1}^N \Delta H^k|} \leq \frac{\max_k |c^k|}{|P_{\text{av}}|} h^p. \quad (68)$$

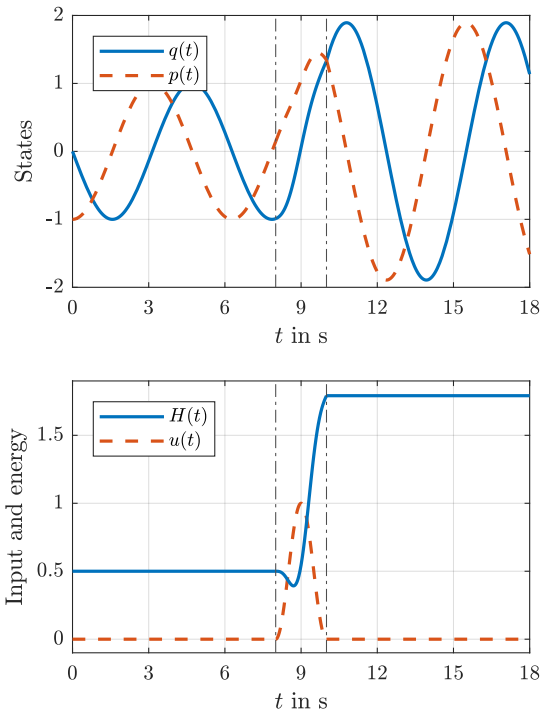


Figure 2: Evolution of states (top), input and energy (bottom) for the forced undamped oscillator

$P_{\text{av}} = \frac{\Delta H_{\text{tot}}}{Nh}$ denotes the average transferred power, and the same estimation of order can be performed for $\tilde{\epsilon}_H$.

The first diagram in Figure 3 nicely shows the orders 2, 4 and 6 of the Gauss-Legendre methods as well as the fact that both approximations $\Delta\tilde{H}^k$ and $\Delta\bar{H}^k$ of supplied and stored energy coincide. (The effect of rounding errors becomes visible at low step sizes in the curve for $s = 3$.) The slopes in the second diagram confirm the orders 4 and 6 of the three-stage Lobatto pair. Although hardly recognizable, the two curves for $\tilde{\epsilon}_H$ and $\bar{\epsilon}_H$ do not match, which is accordance to the computations, see Eq. (61).

5.2. Approximation of dissipated energy

The damped oscillator represents the most basic power-conserving interconnection of a port-Hamiltonian system (the undamped oscillator) with another system (a purely resistive element). This is nicely seen if (62) is combined with the damping injection feedback (64). The differential energy balance in this damped case reads

$$\dot{H} = -ry^2 + yv \leq yv, \quad (69)$$

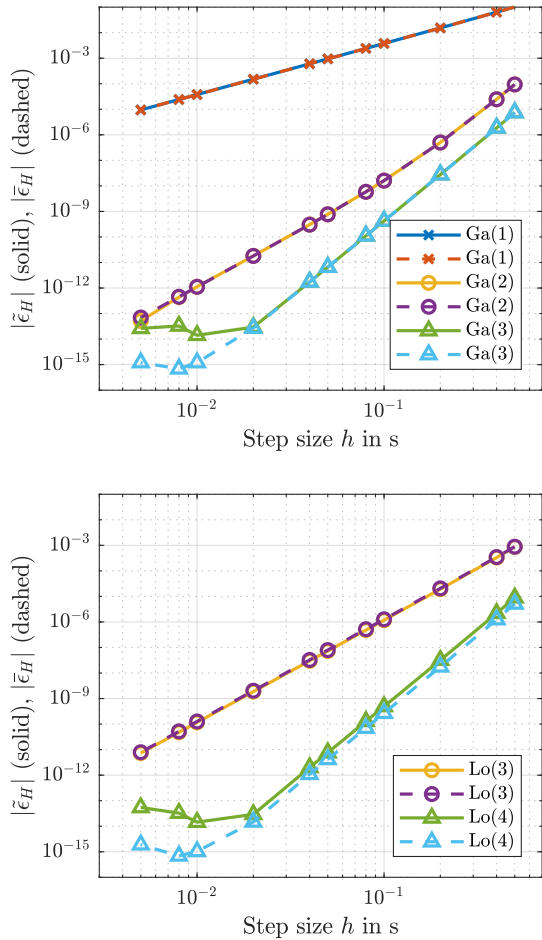


Figure 3: Errors $\tilde{\epsilon}_H$ and $\bar{\epsilon}_H$ of supplied and stored energy for Gauss-Legendre methods, $s = 1, 2, 3$ (top) and Lobatto pairs, $s = 3, 4$ (bottom)

which is the balance of power to the energy storage elements, supplied power and dissipated power. In the discrete-time setting, the damping injection output feedback becomes simply

$$\mathbf{u}^k = -r\mathbf{y}^k + \mathbf{v}^k \quad (70)$$

with discrete input \mathbf{u}^k on the k -th sampling interval as defined in (20) (accordingly for \mathbf{v}^k) and the discrete output \mathbf{y}^k according to (30). By substitution in (37), the approximate energy loss per time step becomes

$$\Delta\tilde{H}^k = -rh(\mathbf{y}^k)^T \mathbf{y}^k + h(\mathbf{y}^k)^T \mathbf{v}^k \leq h(\mathbf{y}^k)^T \mathbf{v}^k. \quad (71)$$

Figure 4 shows the solution of (65) with damping parameter $r = 0.1$ for $v \equiv 0$ and an initial value

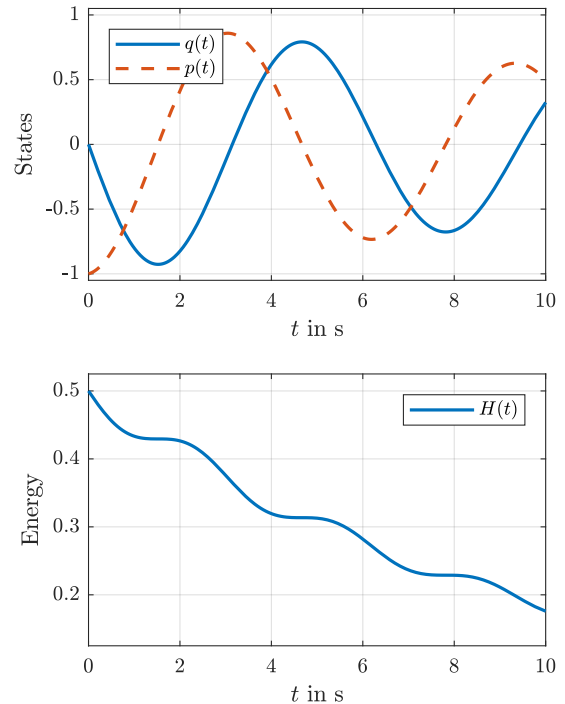


Figure 4: Evolution of the states (top) and the energy (bottom) for the damped oscillator

$\mathbf{x}(0) = [p(0) \ q(0)]^T = [0 \ -1]^T$ on the time interval $[0, 10]$, as well as the monotonous decrease in energy. Figure 5 depicts the magnitude of the relative errors of total dissipated energy according to (67). As in the lossless case, the error plots confirm that the dissipated power is discretized consistently with the order of the underlying geometric numerical integration scheme. This time, the discrepancy between the numerical energy increments $\Delta\tilde{H}^k$ and $\Delta\bar{H}^k$ for the Lobatto pairs, which is of order $\mathcal{O}(h^p)$, is clearly visible in the right diagram.

6. Conclusions

We presented a new definition of discrete-time PH systems, which is based on the approximation of the structure equations and the energy balance of explicit PH systems using the collocation method. By defining a discrete-time Dirac structure, discrete-time constitutive equations and using appropriate geometric numerical integration schemes, the separation between structure, constitutive laws and dynamics, which is a central feature of PH systems, is maintained. The presented work

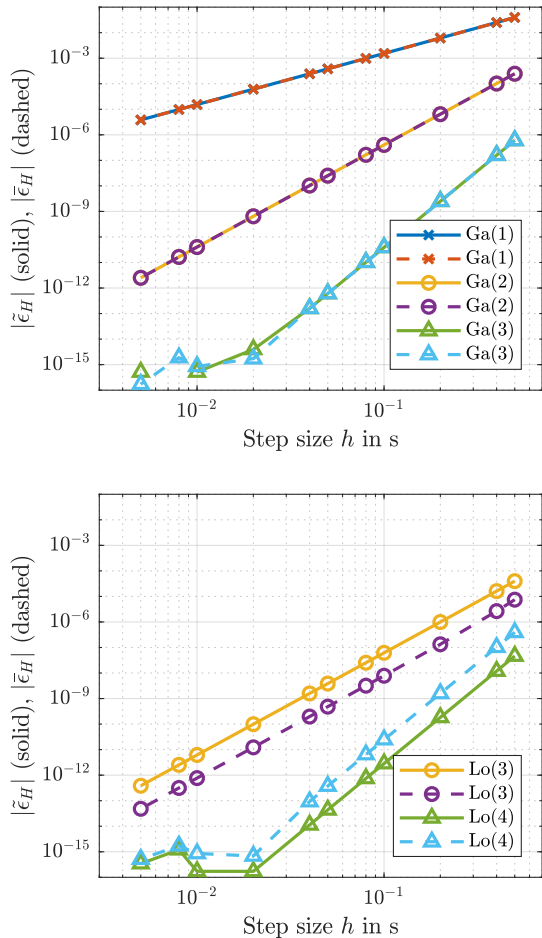


Figure 5: Errors $\tilde{\epsilon}_H$ and $\bar{\epsilon}_H$ of energy flow over the dissipative port and energy loss in the storage elements for Gauss-Legendre methods, $s = 1, 2, 3$ (top) and the Lobatto pair, $s = 3$ (bottom)

extends in a very natural way the notion of geometric/symplectic integration of autonomous Hamiltonian systems to the *open* case (i. e. with power flow over the system boundary) of PH systems.

A focus has been set on proving consistency of the two different numerical energy increments that appear in the context of this definition. The family of implicit Gauss-Legendre schemes – applied to linear PH systems – is the only one for which the approximations of supplied and stored energy match, which leads to an *exact* discrete energy balance of the discrete-time PH approximation. For Lobatto IIIA/IIIB pairs, applied to a linear PH system of partitioned mechanical structure, the discrete energy balance is not exact, but the energy error is

consistent with the numerical integration scheme. The theoretical findings have been illustrated by numerical experiments with the simplest test case of a linear oscillator: The evolution of total energy, which is (i) supplied by an external input or (ii) dissipated based on output damping injection, is approximated up to the order of the underlying integration scheme.

The presented definition of discrete-time PH systems can be exploited in the simulation and numerical analysis of large scale networks. The consistent approximation of energy flows between subsystems and the quantification of their error give important insight that helps to keep track of the quality of simulation results. In the context of network simulation, the numerical approximation of PH DAE systems [13], [14] is of particular interest. Combined with structure-preserving spatial discretization, see e. g. [15], the presented approach contributes to the full discretization of distributed-parameter PH systems. Moreover, the presented work gives rise to reconsider the Control by Interconnection approach, see e. g. [16], for the stabilization of PH systems in discrete time. Finally, more general choices for the time discretization of effort and flow variables are conceivable, which would lead to interesting implicit representations of Dirac structures and, consequently, to implicit discrete dynamics.

References

- [1] B. Leimkuhler, S. Reich, *Simulating Hamiltonian Dynamics*, Vol. 14, Cambridge University Press, 2004.
- [2] E. Hairer, C. Lubich, G. Wanner, *Geometric Numerical Integration: Structure-Preserving Algorithms for Ordinary Differential Equations*, Vol. 31, Springer Science & Business Media, 2006.
- [3] A. Lew, J. E. Marsden, M. Ortiz, M. West, An overview of variational integrators, in: *Finite Element Methods: 1970's and Beyond. Theory and engineering applications of computational methods*, International Center for Numerical Methods in Engineering (CIMNE), Barcelona, 2004, pp. 1–18.
- [4] V. Duindam, A. Macchelli, S. Stramigioli, H. Bruyninx, *Modeling and Control of Complex Physical Systems: The Port-Hamiltonian Approach*, Springer Science & Business Media, 2009.
- [5] L. Gören-Sümer, Y. Yalçın, Gradient based discrete-time modeling and control of Hamiltonian systems, *IFAC Proceedings Volumes* 41 (2) (2008) 212–217.
- [6] S. Aoues, D. Eberard, W. Marquis-Favre, Canonical interconnection of discrete linear port-Hamiltonian systems, in: *52nd IEEE Conference on Decision and Control*, IEEE, 2013, pp. 3166–3171.
- [7] A. Falaize, T. Hélie, Passive guaranteed simulation of analog audio circuits: a port-Hamiltonian approach, *Applied Sciences* 6 (10) (2016) 273.

- [8] V. Talasila, J. Clemente-Gallardo, A. J. van der Schaft, Discrete port-Hamiltonian systems, *Systems & Control Letters* 55 (6) (2006) 478 – 486. doi:10.1016/j.sysconle.2005.10.001.
- [9] E. Celledoni, E. H. Høiseth, Energy-preserving and passivity-consistent numerical discretization of port-Hamiltonian systems, arXiv preprint arXiv:1706.08621.
- [10] P. Kotyczka, L. Lefèvre, Discrete-time port-Hamiltonian systems based on Gauss-Legendre collocation, *IFAC-PapersOnLine* 51 (3) (2018) 125–130.
- [11] A. J. van der Schaft, D. Jeltsema, et al., Port-Hamiltonian Systems Theory: An Introductory Overview, *Foundations and Trends in Systems and Control* 1 (2-3) (2014) 173–378.
- [12] A. J. van der Schaft, *L2-Gain and Passivity Techniques in Nonlinear Control*, 3rd Edition, Springer, 2017.
- [13] A. J. van der Schaft, Port-Hamiltonian differential-algebraic systems, in: *Surveys in Differential-Algebraic Equations I*, Springer, 2013, pp. 173–226.
- [14] C. Beattie, V. Mehrmann, H. Xu, H. Zwart, Port-Hamiltonian descriptor systems, arXiv preprint arXiv:1705.09081.
- [15] P. Kotyczka, B. Maschke, L. Lefèvre, Weak form of Stokes-Dirac structures and geometric discretization of port-Hamiltonian systems, *Journal of Computational Physics* 361 (2018) 442–476. doi:10.1016/j.jcp.2018.02.006.
- [16] R. Ortega, A. J. van der Schaft, F. Castaños, A. Astolfi, Control by Interconnection and standard passivity-based control of port-Hamiltonian systems, *IEEE Transactions on Automatic Control* 53 (11) (2008) 2527–2542.

Acknowledgement

The work was supported by Deutsche Forschungsgemeinschaft (DFG), project KO 4750/1-1, and DFG-ANR (Agence Nationale de la Recherche), project INFIDHEM, ID ANR-16-CE92-0028.